Available online at www.sciencedirect.com

SCIENCE DIRECT®

Journal of Solid State Chemistry 177 (2004) 4167–4174

JOURNAL OF SOLID STATE CHEMISTRY

www.elsevier.com/locate/jssc

Boron–silicon solid solution: synthesis and crystal structure of a carbon-doped boron-rich SiB_n (n~30) compound

Jérome Roger[a], Volodymyr Babizhetskyy[a,b], Jean-François Halet[a], Roland Guérin[a,*]

[a]Laboratoire de Chimie du Solide et Inorganique Moléculaire, Institut de Chimie de Rennes, UMR 6511 CNRS-Université de Rennes 1, Avenue du Général Leclerc, F-35042 Rennes Cedex, France

[b]Max-Planck Institut für Festkörperforschung, Heisenbergstrasse 1, Postfach 800665, D-70569 Stuttgart, Germany

Abstract

The carbon-doped $SiB_{\sim 30}$ compound was obtained during attempts to synthesize by arc-melting boron-rich binaries belonging to the SiB_n solid solution ($13<n<32$). Its crystal structure was determined from X-ray single-crystal intensity data (R-3m, $Z=1$, $a=11.0152(3)$ Å, and $c=23.8625(8)$ Å) and led to the final formula $SiB_{\sim 30}C_{0.35}$. Carbon is incorporated fortuitously in the structure. The boron framework of these phases slightly differs from that encountered in β-boron. The salient characteristic is the partial occupancy of three interstitial boron sites by silicon and one by carbon atoms. This is in contrast with the structurally related compounds such as $SiB_{\sim 36}$, $CrB_{\sim 41}$, or $FeB_{\sim 40}$, in which only two interstitial sites are partially occupied.

Keywords: Silicon; Boron; Crystal structure; X-ray diffraction; Microprobe analysis

1. Introduction

Boron-rich boride silicides are an unfamiliar class of compounds with only a handful of examples known. Indeed, critical assessments of experimental data which are available indicate three binary phases, namely SiB_3, SiB_6, and SiB_n [1]. The first one is encountered within two different forms. One belongs to a solid solution with a compositional spread from $SiB_{2.89}$ and $SiB_{3.65}$ and is identified as α-SiB_3. This rhombohedral phase exists only up to 1270 °C, where it decomposes through a peritectic reaction into the binary phase SiB_6 and B-doped silicon [1]. Recently, an alternative orthorhombic form, referred as β-SiB_3, has been obtained in gallium flux conditions at lower temperature [2]. The second phase SiB_6 is a line compound, which is stable up to 1850 °C, where it decomposes through a peritectic reaction into SiB_n and liquid. The very boron-rich SiB_n is an extended solid solution, the limits of which have been estimated to be about 3 and 6.7 at% Si, thus giving an n value comprised between 13.9 and 32.3 [1]. Previous studies claimed that n ranges from 16 to 26 (3.7–5.9 at% Si) [3,4], confirmed by the single-crystal growth of SiB_{18} [5]. In addition, it is worth mentioning that the phase diagram reveals that silicon and boron dissolve each other up to about 3 at% at 1385 and 2020 °C, respectively. Recent experiments (DTA, X-ray, microprobe, and microhardness) confirm the formation of the B-rich solid phase SiB_n, distinct from, although isotypic with, the solubility of Si in boron [3,4]. This phase SiB_n is obtained through the peritectic reaction: liquid + β-boron solid solution → SiB_n at 2020 °C [1]. Finally, the crystal structure of the very boron-rich binary composition $SiB_{\sim 36}$ (2.7 at% Si), which belongs to the Si-doped β-rhombohedral boron has been known for decades [6].

During investigation on the phase diagram of the ternary Gd–Si–B system [7], we have re-examined the binary systems at the boundaries. In particular, combination of X-ray diffraction (XRD) and electron probe microanalysis (EPMA) experiments on the Si–B system confirmed the above-mentioned phases, except β-SiB_3.

---

*Corresponding author. Fax: +33-2-23-23-67-99.
E-mail address: roland.guerin@univ-rennes1.fr (R. Guérin).

0022-4596/$ - see front matter © 2004 Elsevier Inc. All rights reserved.
doi:10.1016/j.jssc.2004.07.004

Miscibility domain of silicon in boron has also been confirmed. Additionally, a new phase $SiB_{\sim 30}$ (3.2 at% Si) of rhombohedral symmetry, crystallizing in the space group R-3m as β-boron [6,8,9], has been isolated as single crystals in the boron-rich part. Unfortunately, a small amount of carbon is incorporated in the structure (1 at%), which we believe is not necessarily needed to prepare the compound. Neglecting this adventitious carbon inclusion, the phase $SiB_{\sim 30}$ can be considered as the first single-crystal characterized phase belonging to the solid solution SiB_n, ($14<n<32$), [3,4] since $SiB_{\sim 36}$ is a term of the solubility domain of Si-doped β-boron.

Here we describe the synthesis and the crystal structure of this new $SiB_{\sim 30}$ phase, which has been unintentionally doped by carbon. Emphasis is made on the main structural differences with those of β-boron and $SiB_{\sim 36}$. Additionally, the structural relationship with other β-boron derivative phases, such as $CrB_{\sim 41}$, $FeB_{\sim 49}$, $ZrB_{\sim 51}$, $CuB_{\sim 23}$, $ScB_{\sim 28}$, and $MgB_{\sim 20}$ [10–15], in terms of metal occupancy of the β-boron interstitial sites is discussed.

2. Experimental

2.1. Sample preparation

Polycrystalline samples were prepared from powders of pure elements: boron (purity higher than 99.9%) and silicon (>99.999%), both supplied by Strem Chemicals. Prior to the melting of the samples (about 1 g each) in an arc furnace under a Ti/Zr-gettered argon atmosphere, the samples were pressed into pellets. To ensure homogeneity during arc-melting process, the samples were turned over and re-melted several times. Finally, to reach thermodynamic equilibrium, the so-obtained samples were sealed in evacuated silica tubes, heat treated at 1000 °C for 1 month, and subsequently quenched by submerging in cold water.

2.2. Powder diffraction and microprobe analysis

After quenching the samples were cut into several pieces. One part of each sample was pulverized and analyzed by XRD using a powder diffractometer (CPS 120 INEL) equipped with a position-sensitive detector ranging 120° in 2θ. A second part was kept for research of single crystals in the solidified matrix. The last part was embedded in epoxy resin and polished on a nylon cloth using diamond paste of consecutively finer grain sizes (down to 1 μm). To obtain a good surface conductivity, bulk pieces were connected through silver paints. Backscattered electron imaging was done with a Jeol JSM-6301F scanning electron microscope (SEM). Quantitative composition analyses (EPMA) were performed on a Camebax SX 50 using wavelength-dispersive spectroscopy (WDS) of X-rays (GdB_4, Gd_5Si_3, elemental Si and SiB_6 as standards).

Fig. 1. Backscattered electron image of the sample with initial atomic composition B/Si = 90/10. The phase SiB_n corresponds to large and elongated grains (black), while the binary SiB_6 is present as very small grains (gray). SiB_6 results from the peritectic reaction between SiB_n- and Si-rich liquid (white).

Six samples with increasing silicon content from 2.5 to 15 at% were prepared in the boron-rich corner of the Si–B system and examined with SEM and EPMA. For instance, a backscattered electron image of the sample with the initial atomic composition B/Si = 90/10 showed primarily the crystallization of the SiB_n phase which appears as elongated and relatively large grains, as well as the peritectic reaction between this phase and the Si-rich liquid (Fig. 1). The line compound SiB_6 which must be formed through this peritectic reaction at 1850 °C occurs only as very small grains, probably owing to the cooling conditions. About 20 microprobe analyses were done for each annealed sample in order to determine precisely the silicon content. As a result, the minimum and maximum solubility values of silicon in β-boron were found to be 3.2 and 6.4 at%, respectively (standard deviations estimated less than 1 at%). These values are close to those proposed for the solid solution SiB_n in literature (3–6.7 at%) [1]. For the sample B/Si = 90/10, from which single crystals could be extracted, the microanalyses led to the following atomic ratio B/Si = 95.9/4.1.

2.3. Single-crystal XRD

Single-crystal intensity data were collected at room temperature on a Nonius Kappa CCD X-ray area-detector diffractometer using Mo$K\alpha$ radiation ($\lambda = 0.71073$ Å). Only five shiny black platelet-like single crystals could be extracted from the solidified sample having initial atomic composition B/Si = 90/10. Among them, one single crystal was considered of good quality for intensity data collection. The COLLECT program package [16] was used to establish the angular scan conditions (φ and ω scans) used in the data collection.

The structure was solved by direct methods with SIR97 [17] and refined with JANA2000 [18]. Relevant crystal structure and refinement data are given in Table 1. The program DIAMOND was used for the drawings of the structural units [19].

Systematic extinctions together with trigonal Laue symmetry $3m$ allowed three possible space groups, $R32$, $R3m$ and $R\text{-}3m$. In agreement with the literature data for β-rhombohedral boron derivative structures such as $CrB_{\sim41}$ or $FeB_{\sim49}$, the space group $R\text{-}3m$ was retained for structure determination. In order to establish more easily structural relationships, the notation of the atoms for $SiB_{\sim30}$ is given according to that proposed in literature for $SiB_{\sim36}$ [6] and for the $CrB_{\sim41}$-type phases [10–15].

In the first refinement steps, 15 independent boron positions were introduced, among which 13 were found fully occupied. One position *18h* attributed to the atom B13 was found to be slightly deficient ($\tau = 0.742(9)$). Another boron position *36i* was first attributed to boron but showed an abnormally low isotropic temperature factor and a residual electron density in the difference-Fourier map. The best solution was obtained with this site filled but in a statistical occupancy by both boron B1 and silicon Si3 atoms, as in the case of the $SiB_{\sim36}$ structure. It is worth mentioning that the position 18*h* partially occupied by B16 atom in pure β-boron ($\tau = 0.25$) is vacant in this binary structure. Successive difference-Fourier syntheses showed three additional silicon positions, all of them being partially occupied. Indeed, the occupancy of these positions Si1, Si2 and Si4 corresponds to τ values of 0.403(5), 0.033(3), and 0.043(3), respectively. A further difference-Fourier map, after refinement cycles including isotropic-displacement parameters, evidenced a last electron density peak at the position (0.159, 0, $\frac{1}{2}$). This position was first assumed to be occupied by boron ($\tau = 0.252(9)$, $U_{\text{iso}} = 0.013(3)$). However, taking into account the location of the corresponding atoms in the structure (vide infra), this was discarded and it was concluded that this position was either occupied by silicon or carbon. Indeed, carbon could be present as a contamination agent or as an impurity in commercial boron. Moreover, the presence of carbon inclusion in binary β-SiB_3 [2] and the discovery of new borocarbides like $ScB_{17}C_{0.25}$ or $ScB_{15}C_{0.8}$ have been recently mentioned in literature [20–22].

Table 1
Crystal data, intensity collection, and refinement for carbon-doped $SiB_{\sim30}$

Empirical formula	$Si_{10}B_{304}C_{3.5}$
Formula weight ($g\,mol^{-1}$)	3612
Crystal system	Trigonal
Space group	*R-3m*
a (Å)	11.0152(3)
c (Å)	23.8625(8)
V (Å^3)	2507.4(1)
Z, calculated density ($g\,cm^{-3}$)	1; 2.38(1)
Crystal shape	Platelet
Crystal size (mm^3)	$0.065 \times 0.090 \times 0.100$
Linear absorption coefficient (mm^{-1})	0.146
Refinement limits	
θ limits (deg.)	$2<\theta<28$
Data collected	$-14<h<14$
	$-14<k<14$
	$-30<l<30$
Reflections collected	11 170
Independent reflections; R_{int}	751 [$I>1\sigma(I)$]; 0.071
Reflections in refinement	620 [$I>3\sigma(I)$]
Variable parameters	113
Refinement	F
Unweighted R factor (R all data)	0.038 (0.048)
Weighted R_ω factor (R_ω all data)	0.054 (0.058)
[$\omega^{-1} = \sigma^2(F_o)^2 + 0.00221\,F_o^2$]	
Extinction coefficient (*Gaussian isotropic*)	0.6(4)
Scale factor	0.1384(8)
Goodness-of-fit	1.03
Min/max (eÅ^{-3})	−0.36/0.40

The first refinement solution was to consider the position (0.159, 0, $\frac{1}{2}$) to be occupied by silicon ($\tau = 0.070(3)$, $U_{\text{iso}} = 0.020(3)$). However, the close examination of the bond lengths revealed a distance of 1.744(8) Å between this silicon and the boron atom B15, which disagrees with the usual Si–B distances slightly larger than 2 Å. The second time, this distance was judged as quite reasonable for a boron–carbon bond [23–25]. Therefore, the position (0.159, 0, $\frac{1}{2}$) was better assumed to be occupied by carbon ($\tau = 0.195(7)$, $U_{\text{iso}} = 0.006(2)$. In last cycles, the anisotropic-displacement parameters for all boron atoms were introduced in refinement. The final difference-Fourier synthesis did not reveal any significant electron density peak. The formula of this ternary phase, as deduced from the structure refinement, is therefore $Si_{10.08}B_{304.05}C_{3.50}$, that is $SiB_{30.17}C_{0.35}$, giving a corresponding atomic B/Si/C ratio of 95.7/3.2/1.1. Ignoring carbon, this leads to a B/Si ratio of 96.8/3.2, which deviates slightly but remains in the limit of standard deviations with the nominal composition given by EPMA which is 95.9/4.1. It is worth mentioning that the carbon content could not be determined precisely on the samples since EPMA studies always showed the presence of carbon (about 1 at%), even after a short re-polishing of the surface. Indeed, the surface contamination of the sample by carbon is difficult to avoid. For example, on the SiB_6 standard the microprobe analyses when taking into account carbon (graphite and GdB_2C_2 as additional standards) led to the average atomic ratio B/Si/C = 83.47/15.50/1.03. Ignoring carbon, these analyses led to the average atomic B/Si ratio = 84.95/15.05 close to the theoretical 85.71/14.29 ratio. Therefore, following analyses on our bulk samples were performed only on the boron and silicon contents.

Table 2
Positional coordinates, occupancy factors, and equivalent isotropic displacement parameters with their esd's for carbon-doped SiB$_{\sim30}$

Atom	Position	Occupancy	x	y	z	U_{eq} (Å^2)[a]
B1[b]	*36i*	1	0.1691(1)	0.1767(1)	0.17742(4)	0.0153(5)
B2	*36i*	1	0.3183(2)	0.2955(1)	0.12841(6)	0.0119(6)
B3	*36i*	1	0.2611(1)	0.2174(1)	0.41973(6)	0.0107(6)
B4	*36i*	1	0.2353(1)	0.2514(1)	0.34677(6)	0.0101(6)
B5	*18h*	1	0.0542(1)	0.1084(2)	0.94401(9)	0.0084(6)
B6	*18h*	1	0.0858(1)	0.1716(2)	0.01357(8)	0.0087(6)
B7	*18h*	1	0.1101(1)	0.2201(2)	0.88806(8)	0.0112(7)
B8	*18h*	1	0.1701(1)	0.3402(2)	0.02818(8)	0.0093(6)
B9	*18h*	1	0.1304(1)	0.2609(2)	0.76536(8)	0.0116(7)
B10	*18h*	1	0.1020(1)	0.2039(2)	0.69790(8)	0.0090(6)
B11	*18h*	1	0.0565(1)	0.1130(2)	0.32676(9)	0.0088(4)
B12	*18h*	1	0.0897(1)	0.1793(2)	0.39874(8)	0.0093(6)
B13	*18h*	0.742(9)	0.0583(2)	0.1165(3)	0.5542(1)	0.013(1)
B14	*6c*	1	0	0	0.3857(1)	0.0089(8)
B15	*3b*	1	0	0	0.5	0.026(2)
Si1[c]	*6c*	0.403(5)	0	0	0.13254(9)	0.0096(8)
Si2	*18h*	0.033(3)	0.1077(8)	0.215(2)	0.0990(6)	0.010(6)
Si4	*18h*	0.043(3)	0.2036(6)	0.407(1)	0.1731(5)	0.011(4)
C	*18g*	0.195(7)	0.1583(8)	0	0.5	0.006(2)

[a] U_{eq} is defined as one-third of the trace of the orthogonalized U_{ij} tensor.
[b] Mixed position occupied by B1 (82.6%) and Si3 (17.4%) atoms.
[c] The Si atoms, except Si3, as well as the carbon atom have been refined with isotropic thermal parameters.

Final atomic positions and equivalent isotropic-displacement parameters for SiB$_{\sim30}$C$_{0.35}$ are listed in Table 2, and pertinent interatomic distances are given in Table 3.

3. Results and discussion

The carbon-doped SiB$_{\sim30}$ represents a derivative phase of the solid solution SiB$_n$ ($14<n<32$). In spite of the incorporation of a very small amount of carbon in the structure, we believe that it is not needed to prepare the binary SiB$_{\sim30}$. Accordingly, this phase cannot be considered as a carbon-stabilized SiB$_{\sim30}$ phase and for that reason appears as the only phase within the solid solution SiB$_n$, which is structurally described so far. The binary compound SiB$_{14}$ (6.7 at% Si) was proposed earlier by Giese et al. [26], but no experimental atomic positions were given. Recently, Imaï et al. [5] prepared SiB$_{18}$ (i.e., 5.3 at% Si) as single crystal by the floating zone method for electrical properties, but no structure determination was reported . Lattice constants of SiB$_{18}$ ($a = 11.097(1)$ Å, $c = 23.880(4)$ Å) are slightly larger than the ones determined for SiB$_{\sim30}$ ($a = 11.0152(3)$ Å, $c = 23.8625(8)$ Å), in agreement with a higher Si content.

Moreover, the crystal structure of SiB$_{\sim30}$ is strongly related to those of SiB$_{\sim36}$ (Si/B = 8.4/305.5, i.e., 2.7 at% Si) and β-boron, since the space group is the same and the unit-cell parameters are nearly similar, i.e., $a = 11.01(1)$ Å, $c = 23.90(2)$ Å for SiB$_{\sim36}$ [6] and $a = 10.9270(8)$ Å, $c = 23.828(8)$ Å for β-boron [9].

The crystal structure of SiB$_{\sim30}$ can be simply described knowing that of β-boron, previously reported by Hoard et al. [27]. The boron framework is made of B$_6$ half-icosahedra, B$_{12}$ icosahedra and single boron atoms (B15). The assemblage of 12 B$_6$ units gives rise to a large quasi-spherical B$_{72}$ cage, which is centered by a B$_{12}$ icosahedron leading to a B$_{84}$ unit (Fig. 2a) located at the origin and with its three-fold axis along the c-direction of the hexagonal unit cell (Fig. 2b). Moreover, three B$_{12}$ icosahedra condense by sharing 10 atoms to generate a B$_{28}$ unit (Fig. 2a). The B$_{84}$ and B$_{28}$ units stack along the [001] direction with the sequence –B$_{84}$–B$_{28}$–B$_{28}$–. The B$_{28}$ units are covalently bound through the single boron atom B$_{15}$, wholly independent and located along the c-axis, whereas B9 atoms link the B$_{28}$ units and B$_{84}$ cages together (Fig. 2b). It can be noted that each B9 atom is not isolated since it belongs actually to a B$_6$ half-icosahedron, which is anchored to the B$_{84}$ unit. Moreover, each B$_{84}$ unit is connected to six B$_{28}$ units, through sharing of B$_6$ half-icosahedra. The six B$_{28}$ units in turn are arranged around the B$_{84}$ unit in such a way that three B$_{28}$ units are down- and three up-pointed (Fig. 2c). Inversely, every B$_{28}$ unit is linked to three B$_{84}$ units. Additionally, the B$_{28}$ units are linked to each other through interunit B–B bonds.

Interstitial boron sites are present in the structure SiB$_{\sim30}$. These sites are labeled $A1$, $A2$ and D in the literature [6,15]. In addition, a new site has been found,

Table 3
Interatomic distances (Å) (<2.20 Å) and their esd's for carbon-doped $SiB_{\sim 30}$

B1–B1	2.031(2)	B6–B5	1.766(3)	B13–2B3	1.790(4)
B1–B1	1.778(2)	B6–2B5	1.755(4)	B13–2B12	1.877(4)
B1–B2	1.905(2)	B6–2B6	1.760(4)	B13–2B13	1.925(4)
B1–B2	1.895(2)	B6–B8	1.646(3)	B13–B14	1.816(4)
B1–B7	1.926(3)	B6–Si2	2.08(1)	B13–B15	1.705(3)
B1–B9	1.914(3)			B13–2C	1.609(5)
B1–Si1	2.186(1)	B7–2B1	1.926(2)	B13–Si4	1.99(1)
B1–Si2	2.10(1)	B7–2B2	1.813(3)		
		B7–B5	1.709(3)	B14–3B11	1.771(3)
		B7–B9	1.799(3)	B14–3B12	1.739(2)
B2–B1	1.905(2)	B7–Si1	2.157(2)	B14–3B13	1.816(4)
B2–B1	1.895(2)	B7–2Si2	2.10(2)		
B2–B2	1.848(2)				
B2–B3	1.720(3)	B8–2B3	1.798(3)	B15–6B13	1.705(3)
B2–B7	1.813(3)	B8–2B4	1.747(3)	B15–6C	1.744(6)
B2–B9	1.859(4)	B8–B6	1.646(3)		
B2–Si2	2.146(9)	B8–B10	1.838(3)	Si1–6B1	2.186(2)
		B8–Si2	2.07(1)	Si1–3B5	2.099(3)
				Si1–3B7	2.157(2)
B3–B2	1.720(3)			Si1–3Si2	2.20(2)
B3–B3	1.913(3)	B9–2B1	1.914(3)		
B3–B4	1.833(2)	B9–2B2	1.859(3)	Si2–2B1	2.10(1)
B3–B8	1.798(3)	B9–B7	1.799(3)	Si2–2B2	2.15(2)
B3–B12	1.789(3)	B9–B10	1.699(3)	Si2–2B3	2.07(2)
B3–B13	1.790(3)			Si2–2B5	2.05(2)
B3–C	2.154(3)	B10–2B4	1.843(3)	Si2–B6	2.08(1)
B3–Si2	2.07(2)	B10–B8	1.838(3)	Si2–2B7	2.10(2)
		B10–B9	1.699(3)	Si2–B8	2.07(1)
B4–B3	1.833(2)	B10–2B11	1.788(4)	Si2–Si1	2.20(2)
B4–B4	1.689(2)				
B4–B8	1.747(4)	B11–2B4	1.852(3)	Si4–B13	1.99(1)
B4–B10	1.843(3)	B11–2B10	1.788(3)	Si4–2C	1.31(2)
B4–B11	1.852(3)	B11–2B11	1.868(3)		
B4–B12	1.862(3)	B11–B12	1.830(3)	C–2B3	2.154(4)
		B11–B14	1.771(3)	C–2B13	1.609(5)
B5–2B5	1.791(3)			C–B15	1.744(8)
B5–B6	1.766(3)	B12–2B3	1.789(3)	C–2C	1.75(1)
B5–2B6	1.755(3)	B12–2B4	1.862(2)	C–2Si4	1.31(2)
B5–B7	1.709(3)	B12–B11	1.830(3)		
B5–Si1	2.099(3)	B12–2B13	1.877(4)		
B5–2Si2	2.05(2)	B12–B14	1.739(2)		

namely the site *H*. All these sites can be easily visualized looking along the *c*-direction (Fig. 2d). Indeed, they are partially occupied by the Si1, Si2, Si4 and C atoms, respectively (Table 4). The Si1 and Si2 atoms are located along the *c*-direction above and below the B_{12} icosahedron encapsulated inside the B_{72} cage. Their coordination number (CN) is 15 and 13, respectively. Si1 has 12 B neighbors at 2.10–2.19 Å and three Si neighbors (when present) at 2.20 Å. Si2 is also surrounded by 12 B atoms at 2.05–2.15 Å but by only one Si atom (when present) at 2.20 Å (Table 3). The Si4 and C atoms are located between two subsequent B_{28} units along the *c*-direction in the coordination sphere of B15 (Fig. 2d). Their CN within the limit of 2.20 Å is smaller. Indeed, only one B atom at 1.99 Å and two C atoms (when present) at 1.31 Å are coordinated to Si4, whereas five B atoms at 1.61–2.15 Å, two Si atoms (when present) at 1.31 Å, and two C atoms at 1.75 Å induce a maximum CN of 9 for the C atom. Coordination polyhedra around the Si and C atoms are in turn difficult to define, since their occupancy factors are significantly small.

At first sight, the crystal structure of $SiB_{\sim 30}$ is not far from the one of $SiB_{\sim 36}$, determined by Vlasse and Viala [6], which is also close to that of β-boron, as far as the boron framework is concerned [26]. A comparison of the binary structures $SiB_{\sim 30}$ and $SiB_{\sim 36}$ with that of β-boron indicates that the main difference arises from the absence of the B16 atom in the former compounds. This vacant position is probably not important for the stability of the boron framework in these phases. Moreover, one boron position is partially substituted by silicon in both binaries, namely the (B1, Si3) atom. It

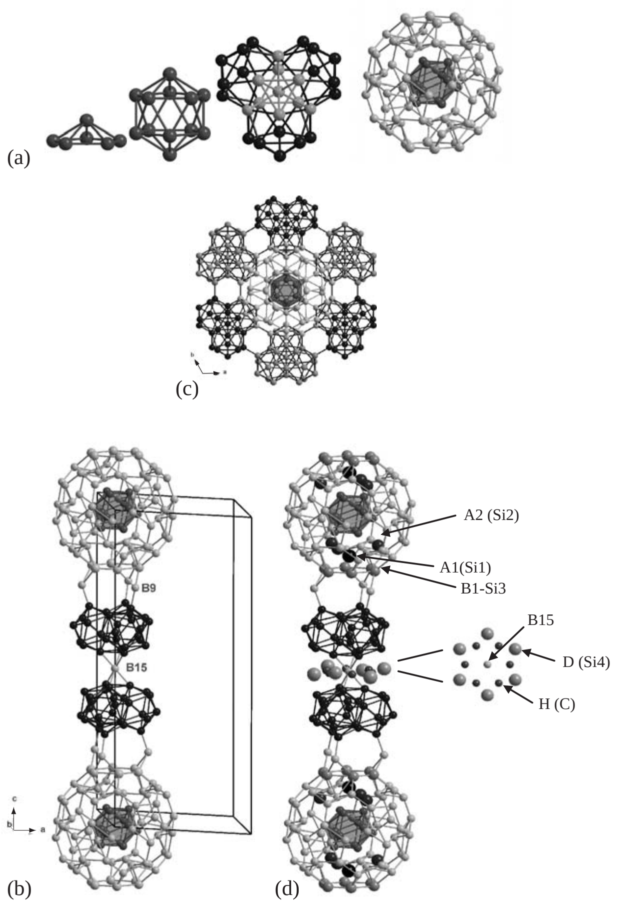

Fig. 2. Structural representation of carbon-doped SiB$_{\sim30}$: (a) B_6 half-icosahedron, B_{12} icosahedron, condensed B_{28}, and B_{84} units; (b) stacking of the B_{28} and B_{84} units along the *c*-axis corresponding to the common β-boron framework; (c) linkage of the B_{84} unit with its six neighboring B_{28} units in projection onto the (001) plane; and (d) representation along the *c*-axis of the interstitial sites partially occupied by silicon and carbon atoms in the structure.

is worth mentioning that, with the exception of the boron position B13 ($\tau \sim 0.75$), all the other positions are fully occupied in all the three compounds. In addition to the boron framework, and with the exception of the C atoms present in a new site *H*, the structure SiB$_{\sim30}$ contains three additional crystallographically distinct Si atoms which, as said above, partially occupy the interstitial sites *A*1, *A*2, and *D*. This differs with SiB$_{\sim36}$, in which only the two first sites *A*1 and *A*2 are found to be partially occupied, with occupancy factors very close to those in SiB$_{\sim30}$ (Table 4). The increase in silicon content in the latter with respect to the former leads to a partial occupancy of the extra site *D* by the Si4 atoms. Probably, the occupancy factor of this site is higher within the solid solution SiB$_n$, when *n* value is decreasing.

Interestingly, comparison of SiB$_{\sim30}$ with β-boron derivative phases such as CrB$_{\sim41}$ or FeB$_{\sim49}$ shows that the Si1 and Si4 atoms partially occupy the same sites *A*1 and *D* as chromium or iron atoms in the latter compounds [10,12] (Table 4). For instance, sites *A*1 (0, 0, 0.132) and *D* (0.203, 0.406, 0.174) are occupied by 51 and 19 at% Fe in FeB$_{\sim49}$, while their occupancy in SiB$_{\sim30}$ is 40.3(5) and 4.3(3) at% Si, respectively. On the contrary, site *A*2 (0.108, 0.215, 0.100), which is never occupied by a metal atom in the CrB$_{\sim41}$-type structures is now very slightly occupied by Si2 (3.3(3) at%).

In contrast to site *D*, partially occupied in the CrB$_{\sim41}$-type structures, occupancy of site *H* (0.158, 0, $\frac{1}{2}$) has never been mentioned previously in the literature (Table 4). Its position is close to that of site *D*, both being in the close environment of B15 (Fig. 2d). Consequently, the Si4–C distance of 1.31 Å is too short for a silicon–carbon bond, but in relation with the small

Table 4
Sites with their occupancy factors in C-doped SiB$_{\sim30}$ and in β-boron derivative structures

Labeling and approximate coordinates	β-B	SiB$_{\sim36}$[a]	C-doped SiB$_{\sim30}$[b]	FeB$_{\sim49}$	CrB$_{\sim41}$	CuB$_{\sim23}$	ZrB$_{\sim51}$	ScB$_{\sim28}$	MnB$_{\sim23}$	MgB$_{\sim20}$
*A*1		Si1	Si1	Fe1	Cr1	Cu1			Mn1	
0, 0, 0.135		46%	40.30%	51%	72%	8%			26%	
*A*2		Si2	Si2							
0.108, 0.216, 0.100		4.80%	3.30%							
D			Si4	Fe2	Cr2	Cu2	Zr2	Sc2	Mn2	Mg
0.205, 0.411, 0.174			4.30%	19%	18%	22%	28%	31%	43%	48%
E						Cu3	Zr3	Sc3	Mn3	Mg
0, 0, 0.245						61%	18%	73%	66%	91%
F										Mg
0.391, 0, 0										9%
G	B16					B16	B16			
0.055, 0.109, 0.117	25%					13%	15%			
H			C							
0.158, 0, 0.5			19.50%							

[a] Data from Vlasse and Viala [6].
[b] Our study.

occupancy factors (Table 3). This distance suggests that both sites *D* and *H* cannot be occupied at the same time by these atoms. On the other hand, the partial occupancy of the *A*1, *A*2, and *D* sites by silicon hardly depends on the dimension and symmetry of the sites. The covalent radius of silicon (1.17 Å), less than the metallic radius of transition elements such as iron (1.26 Å), enables silicon atoms to be inserted in smaller holes. The smallest one is probably the new site *H*, which accommodates one-fifth of a carbon atom (covalent radius of carbon 0.77 Å). In the same manner, it is worth mentioning that the absence of the B16 atom in the β-boron derivative structures depends on the adding of interstitial atoms in the *A*1-type hole. Indeed, this is due to the very small distance between B16 and the center of the *A*1 hole (~1.12 Å). The only exception is observed in the binary compound $CuB_{\sim 23}$, where the *A*1 site is mentioned to be partially occupied by a copper atom but with a low occupancy factor ($\tau = 0.08$) (Table 4).

4. Conclusion

We have reported here the synthesis and the characterization of the new carbon-doped $SiB_{\sim 30}$ phase. From our opinion, this carbon inclusion is adventitious and has no influence for stabilizing the new binary. Therefore, $SiB_{\sim 30}$ can be considered as belonging to the solid solution SiB_n ($14 < n < 32$), which must be viewed distinct, although almost isotypic, from the solubility domain of Si in β-boron. The crystal structure determined on single crystal shows that the boron framework of this compound slightly differs from that encountered in β-boron. The salient characteristic of this binary structure results from the partial occupancy of three interstitial boron sites by silicon atoms, two of which with very low occupancy factors ($\tau = 0.033$ and 0.043). Partial occupancy of three interstitial boron sites is in contrast with the structurally related compounds such as $SiB_{\sim 36}$, which belongs to the solubility domain of silicon in β-boron, and in which only two interstitial sites are partially occupied. It differs as well from $CrB_{\sim 41}$ or $FeB_{\sim 40}$, in which only one interstitial site is partially occupied. Location of carbon ($\tau = 0.195$) in the additional boron site *H* must be considered as adventitious.

The binary phase SiB_{18}, the composition of which is not far from that of $SiB_{\sim 30}$, is a *p*-type semiconductor with an electrical conductivity of about $1\,\Omega^{-1}\,cm^{-1}$ at room temperature [5]. Knowing the interest of boron–silicon compounds for their potential thermoelectric properties, future investigations of the physical properties of SiB_n ($n \sim 30$) will be performed.

4.1. Supporting information available

Further details of the crystal structure investigation can be obtained from the Fachinformationszentrum Karlsruhe, 76344 Eggenstein-Leopoldshafen, Germany (fax: +49-7247-808-666; e-mail: crysdata@fiz.karlsruhe.de), on quoting the depository number CSD-413978.

Acknowledgment

V. Babizhetskyy is grateful to the Centre National de la Recherche Scientifique (France) for a research grant (2001–2002). The authors also thank J. Bauer for fruitful discussions and T. Roisnel (CDIFX, Université de Rennes 1) for X-ray intensity data collection as well as J.C. Jegaden, J. Le Lannic (CMEBA, Université de Rennes 1), and M. Bohn (IFREMER, Brest) for their assistance in SEM and EPMA studies.

References

[1] T.B. Massalski, Binary Alloy Phases Diagrams, 2nd ed., ASM, Materials Park, OH, 1990.
[2] J.R. Salvador, D. Blic, S.D. Mahanti, M.G. Kanatzidis, Angew. Chem. 42 (2003) 1929.
[3] B. Armas, G. Male, D. Salanoubat, C. Chatillon, M. Allibert, J. Less-Common Met. 82 (1981) 245.
[4] G. Male, D. Salanoubat, Rev. Int. Hautes Temp. Refract. 18 (1981) 109.
[5] M. Imai, T. Kimura, K. Sato, T. Hirano, J. Alloys Compds. 306 (2000) 197.
[6] M. Vlasse, J.C. Viala, J. Solid State Chem. 37 (1981) 181.
[7] V. Babizhetskyy, J. Roger, S. Députier, R. Jardin, J. Bauer, R. Guérin, J. Solid State Chem. 177 (2004) 415.
[8] A.J. Crespo, L.E. Tergenius, T. Lundstrom, J. Less-Common Met. 77 (1981) 147.
[9] B. Callmer, Acta Crystallogr. B 33 (1977) 1951.
[10] S. Andersson, T. Lundström, J. Solid State Chem. 2 (1970) 603.
[11] B. Callmer, L.-E. Tergenius, J.O. Thomas, J. Solid State Chem. 26 (1978) 275.
[12] B. Callmer, T. Lundström, J. Solid State Chem. 17 (1976) 165.
[13] B. Callmer, J. Solid State Chem. 23 (1978) 391.
[14] S. Brutti, M. Colapietro, G. Balducci, L. Barba, P. Manfrinetti, A. Palenzona, Intermetallics 10 (2000) 811.
[15] K. Soga, A. Oguri, S. Araake, M. Terauchi, A. Fujiwara, K. Kimura, J. Solid State Chem. 177 (2004) 498.
[16] Nonius Kappa CCD Program Package COLLECT, DENZO, SCALEPACK, Nonius BV, Delft, The Netherlands, 1998.
[17] A. Altomare, M.C. Burla, M. Camalli, B. Carrozzini, G.L. Cascarano, C. Giacovazzo, A. Guagliardi, A.G.G. Moliterni, G. Polidori, R. Rizzi: SIR97, A new tool for crystal structure determination and refinement, J. Appl. Crystallogr. 32 (1999) 115.
[18] V. Petricek, M. Dusek, JANA2000, Program for Crystal Structure Refinement, Institute of Physics, Academy of Sciences of the Czech Republic, Praha, 2000.
[19] K. Brandenburg, Diamond, Version 2.0, 1998.
[20] T. Tanaka, J. Alloys Compds. 270 (1998) 132.
[21] Y. Shi, A. Leithe-Jasper, T. Tanaka, J. Solid State Chem. 148 (1999) 250.

[22] A. Leithe-Jasper, L. Bourgeois, Y. Michiue, Y. Shi, T. Tanaka, J. Solid State Chem. 154 (2000) 130.
[23] J. Bauer, J.-F. Halet, J.-Y. Saillard, Coord. Chem. Rev. 170–180 (1998) 723 and references therein.
[24] J.R. Salvador, D. Bilc, S.D. Mahanti, M.G. Kanatzidis, Angew. Chem. Int. Ed. 41 (2002) 844.
[25] B. Albert, K. Schmitt, Chem. Commun. (1998) 2373.
[26] R.F. Giese Jr., J. Economy, V.I. Matkovich, Z. Kristallogr. 122 (1965) 144.
[27] J.L. Hoard, D.B. Sullenger, C.H.L. Kennard, R.E. Hughes, J. Solid State Chem. 1 (1970) 268.